Supplemental Figure 1

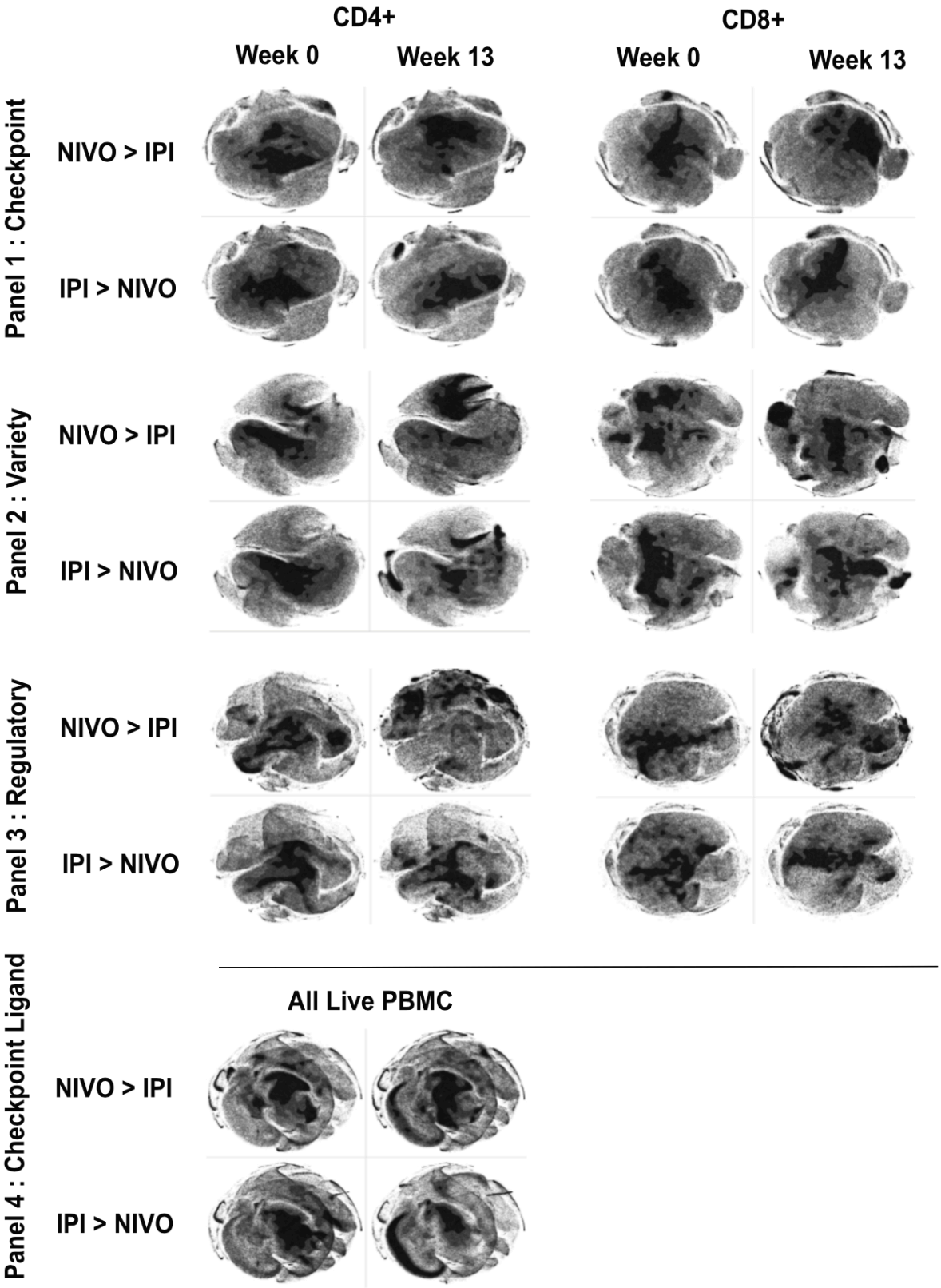

Supplemental Figure 1. tSNE-based visualizations of immunophenotyping data. tSNE analyses are shown for the indicated flow panels, patient groups, and sample time point.

Supplemental Figure 2

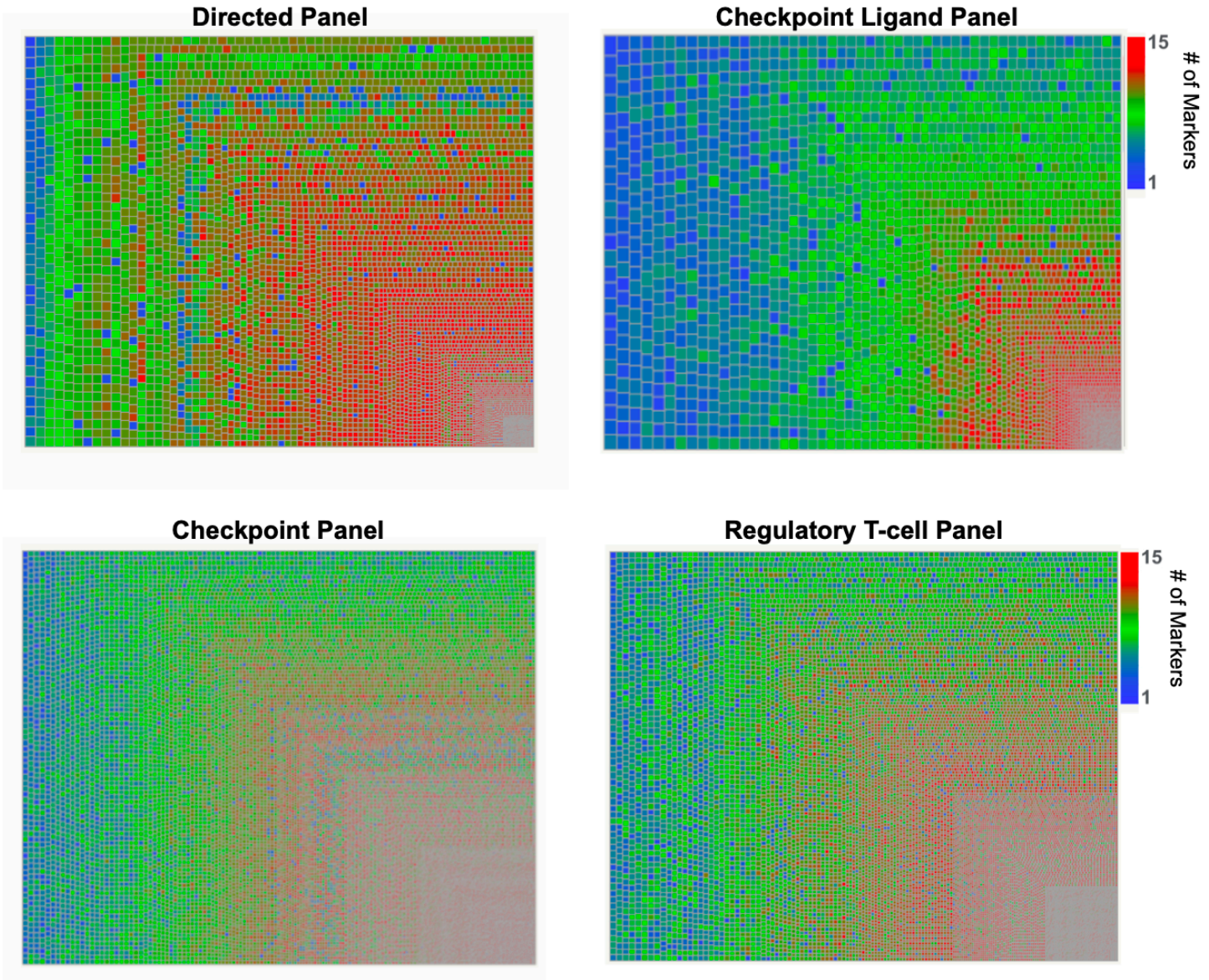

Supplemental Figure 2. Mosaic plots of immunophenotype complexity and frequency. Mosaic plots for each antibody panel, in which the frequency of each immunophenotyped defined by combinatorics is depicted by the size of its tile. The immunophenotypes are arranged such that the most frequent populations are in the upper left corner of the graphic, while the least frequent are in the lower right corner. The color scale denotes the number of markers used to describe each immunophenotype.

Supplemental Figure 3

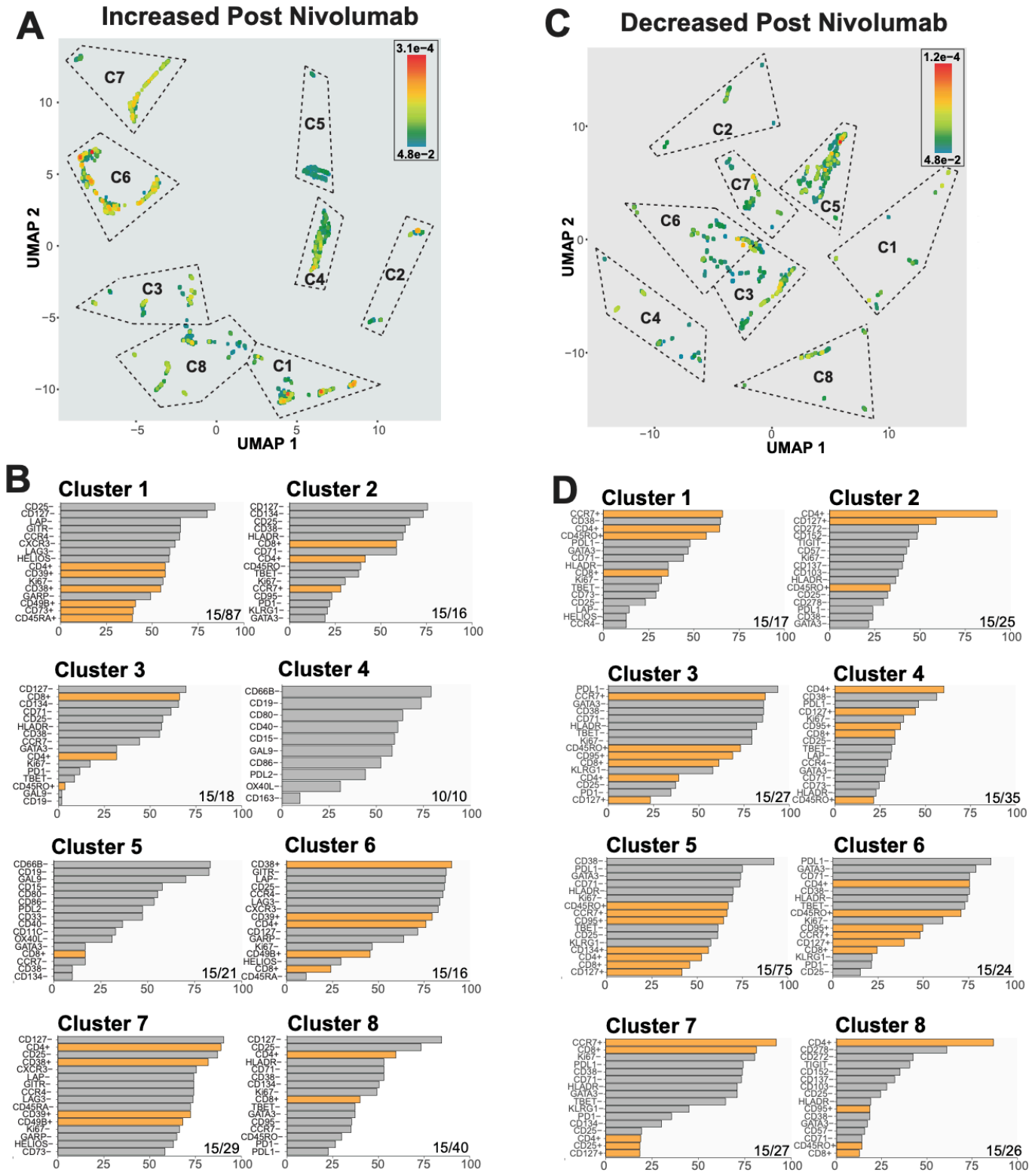

Supplemental Figure 3. Changes in peripheral immunophenotypes post nivolumab. (A) Immunophenotypes significantly increased post nivolumab ($p<0.05$, Wilcoxon signed-rank test) were reduced to a two-dimensional graph by Uniform Manifold Approximation and Projection (UMAP) by using frequency values for all patient samples as n-dimension variables. Clusters were determined by K-Means. Each dot represents a significant immunophenotype and is colored by the p-value. **(B)** The frequency for the top markers appearing in each cluster are graphed. Positive markers (e.g. CD38+) are shown in orange bars and negative markers (e.g. CD38-) are shown in grey bards. The total number of markers appearing is shown in

the bottom right of each panel. **(C, D)** Immunophenotypes significantly decreased post nivolumab are likewise graphed and the cluster phenotypes shown.

Supplemental Figure 4

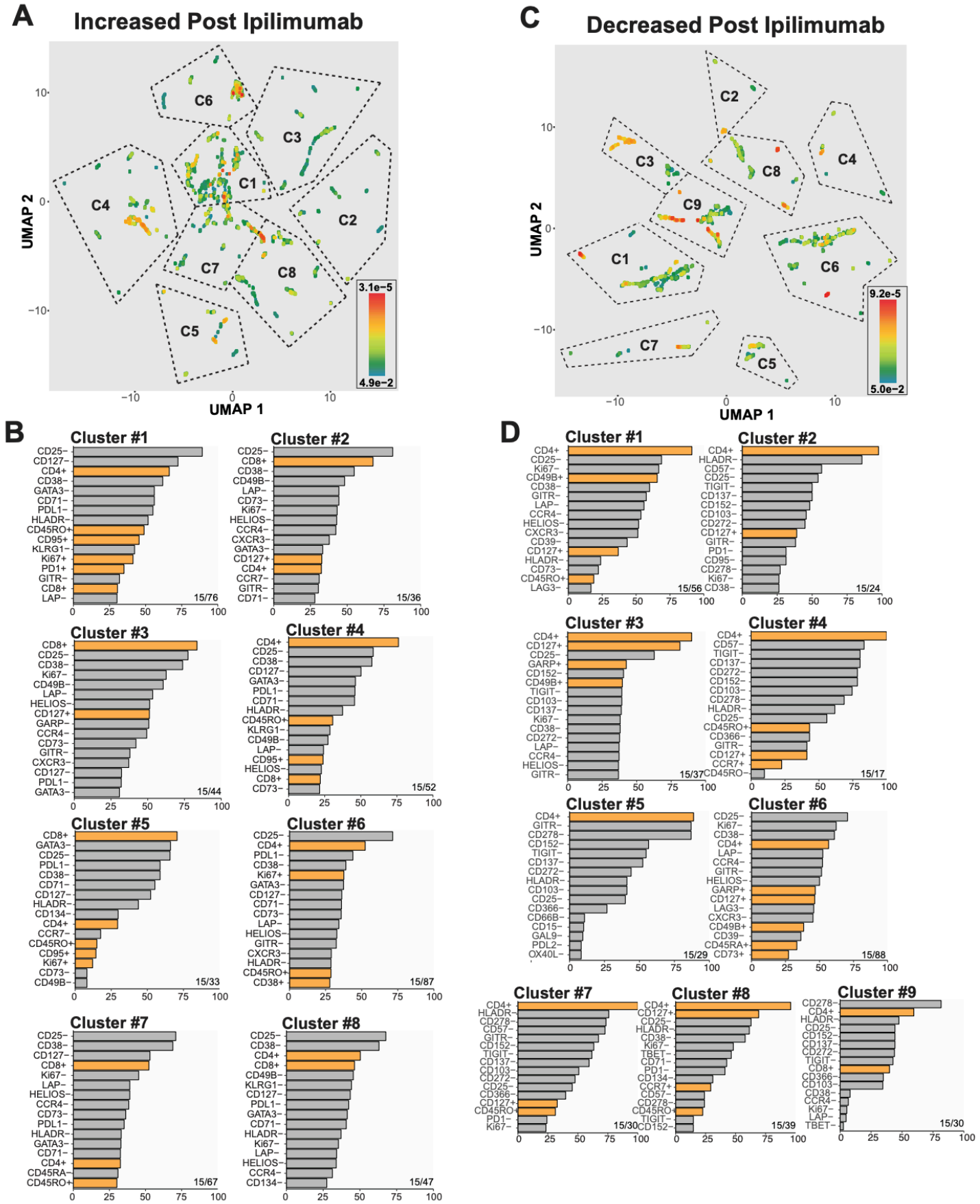

Supplemental Figure 4. Changes in peripheral immunophenotypes post ipilimumab. (A) Immunophenotypes significantly increased post ipilimumab ($p<0.05$, Wilcoxon signed-rank test) were reduced to a two-dimensional graph by UMAP by using frequency values for all patient samples as n-dimension variables. Clusters were determined by K-Means. Each dot represents a significant immunophenotype and is colored by the p-value. **(B)** The frequency for the top markers appearing in each cluster are graphed. Positive markers are shown in orange bars and negative markers are shown in grey bards. The total number of markers appearing is shown in the bottom right of each panel. **(C, D)** Immunophenotypes significantly decreased post ipilimumab are likewise graphed and the cluster phenotypes shown.

Supplemental Figure 5

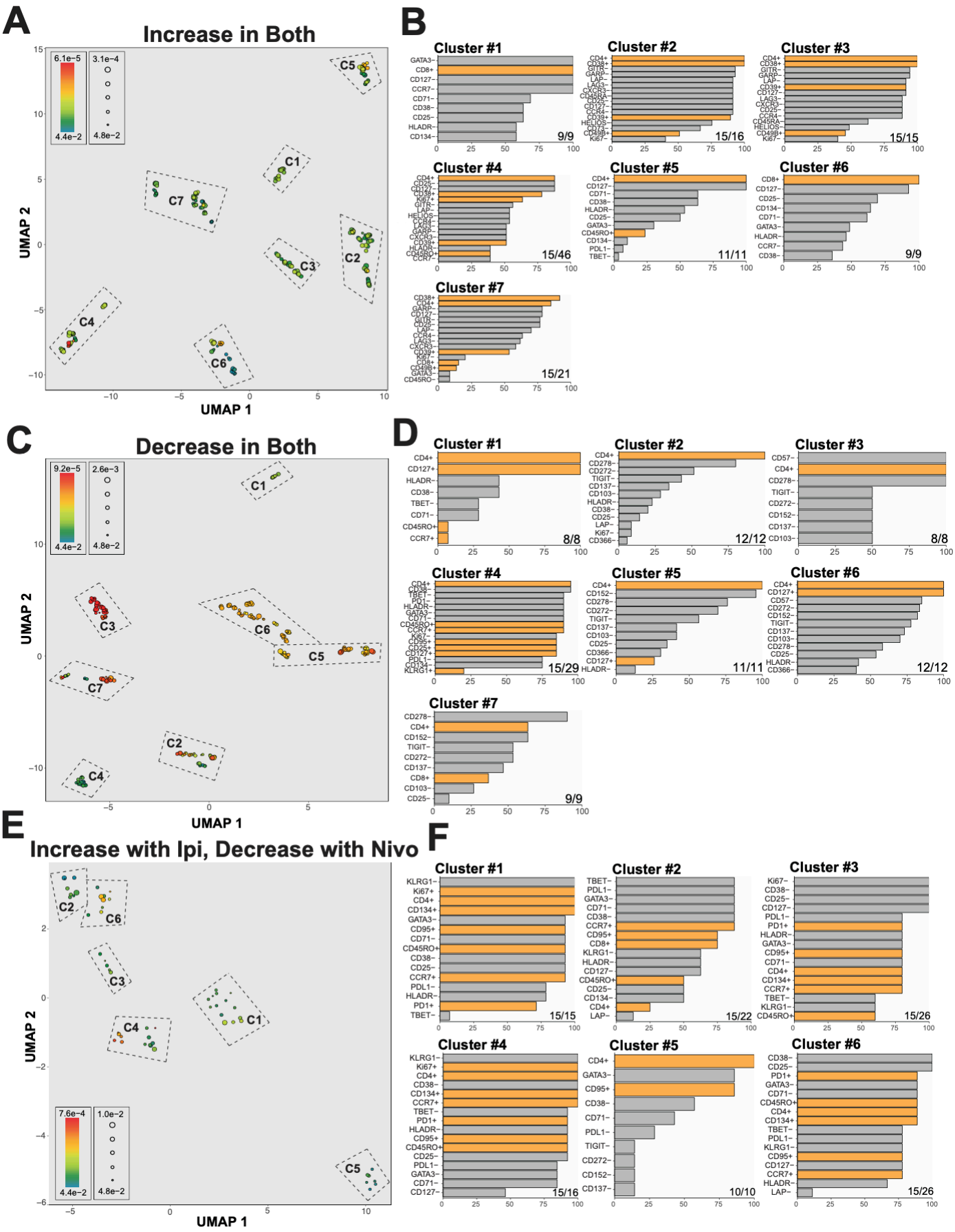

Supplemental Figure 5. Overlap in nivolumab- and ipilimumab-induced peripheral immunophenotypic changes. (A) The 281 immunophenotypes found to be significantly increasing both post ipilimumab and post nivolumab ($p<0.05$, Wilcoxon signed-rank test) were reduced to a two-dimensional graph by UMAP by using frequency values for all patient samples as n-dimension variables. Clusters were determined by K-Means. Each dot represents a significant immunophenotype and is colored by the p-value of change after nivolumab treatment and is sized by the p-value of change after ipilimumab treatment. **(B)** The frequency for the top markers appearing in each cluster are graphed. Positive markers are shown in orange bars and negative markers are shown in grey bards. The total number of markers appearing is shown in the bottom right of each panel. **(C, D)** The 244 immunophenotypes significantly decreased both post nivolumab and post ipilimumab are likewise graphed and the cluster phenotypes shown. **(E, F)** The 56 immunophenotypes significantly decreased both post nivolumab and increased post ipilimumab are likewise graphed and the cluster phenotypes shown.

Supplemental Figure 6

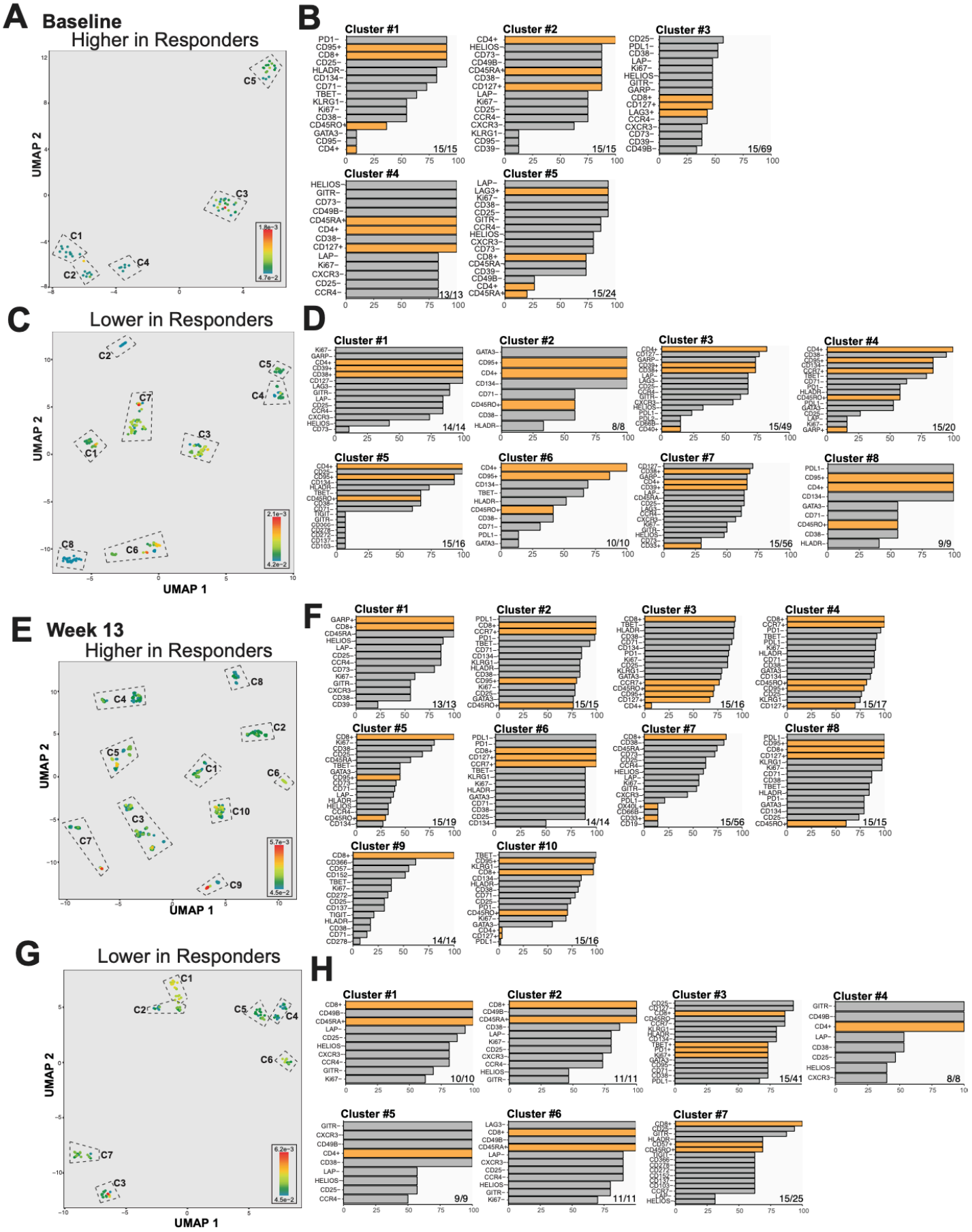

Supplemental Figure 6. Biomarkers associated with patient response and survival after sequential nivolumab>ipilimumab therapy. (A) Baseline immunophenotypes significantly higher in nivolumab>ipilimumab responding patients relative to progressing patients were reduced to a two-dimensional graph by UMAP by using frequency values for all patient samples as n-dimension variables. Clusters were determined by K-Means. Each dot represents an immunophenotype and is colored by p-value. **(B)** The frequency for the top markers appearing in each cluster are graphed. Positive markers are shown in orange bars and negative markers are shown in grey bards. The total number of markers appearing is shown in the bottom right of each panel. **(C, D)** Baseline immunophenotypes significantly lower in nivolumab>ipilimumab responding patients are likewise graphed and the cluster phenotypes shown. **(E,F)** Post-nivolumab immunophenotypes significantly higher in nivolumab>ipilimumab responding patients are likewise graphed and the cluster phenotypes shown. **(G, H)** Post-nivolumab immunophenotypes significantly lower in nivolumab>ipilimumab responding patients are likewise graphed and the cluster phenotypes shown.

Supplemental Figure 7

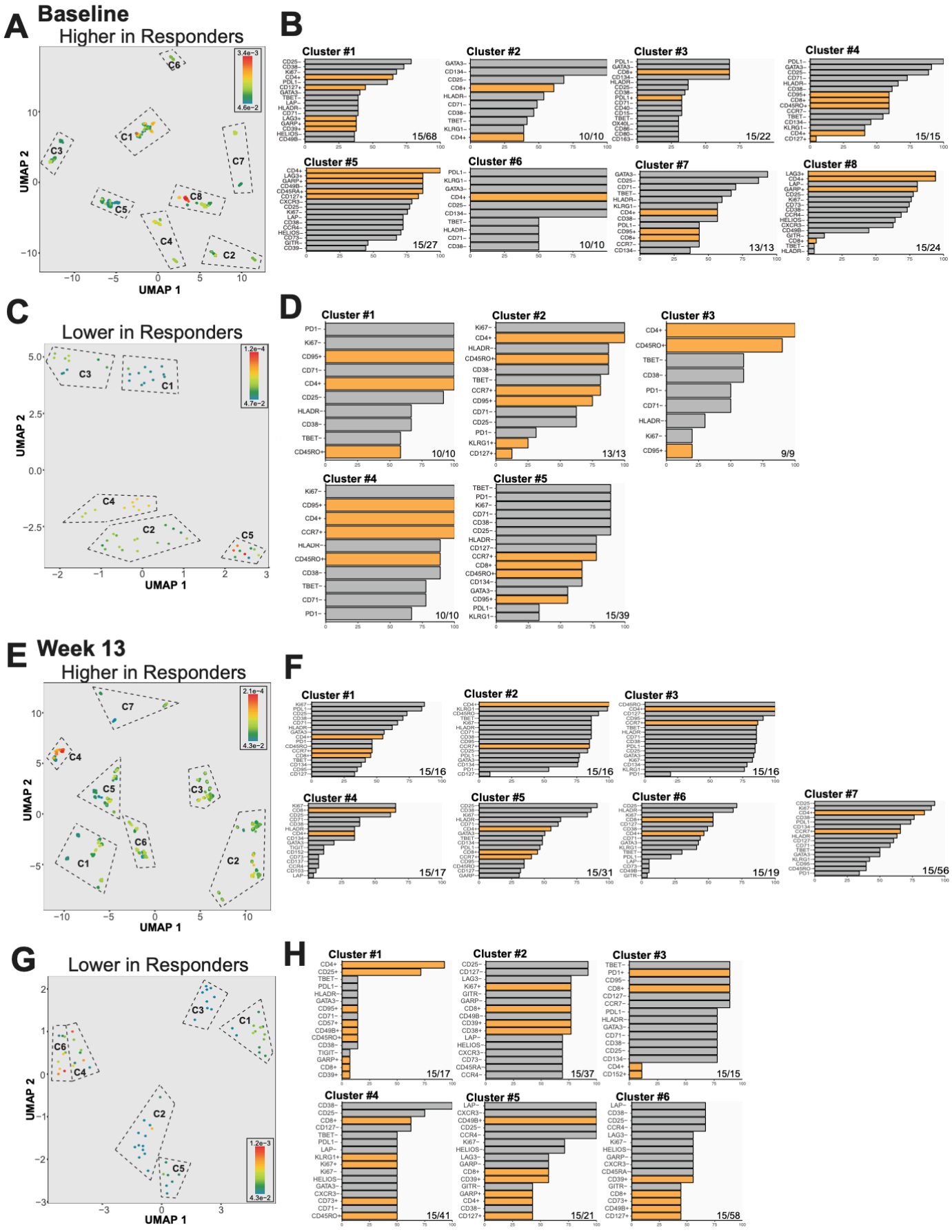

Supplemental Figure 7. Biomarkers associated with patient response and survival after sequential ipilimumab>nivolumab therapy. (A) Baseline immunophenotypes significantly higher in ipilimumab>nivolumab responding patients relative to progressing patients were reduced to a two-dimensional graph by UMAP by using frequency values for all patient samples as n-dimension variables. Clusters were determined by K-Means. Each dot represents an immunophenotype and is colored by p-value. **(B)** The frequency for the top markers appearing in each cluster are graphed. Positive markers are shown in orange bars and negative markers are shown in grey bards. The total number of markers appearing is shown in the bottom right of each panel. **(C, D)** Baseline immunophenotypes significantly lower in ipilimumab-nivolumab responding patients are likewise graphed and the cluster phenotypes shown. **(E, F)** Post-ipilimumab immunophenotypes significantly higher in ipilimumab>nivolumab responding patients are likewise graphed and the cluster phenotypes shown. **(G, H)** Post-ipilimumab immunophenotypes significantly lower in ipilimumab>nivolumab responding patients are likewise graphed and the cluster phenotypes shown.

Supplemental Figure 8

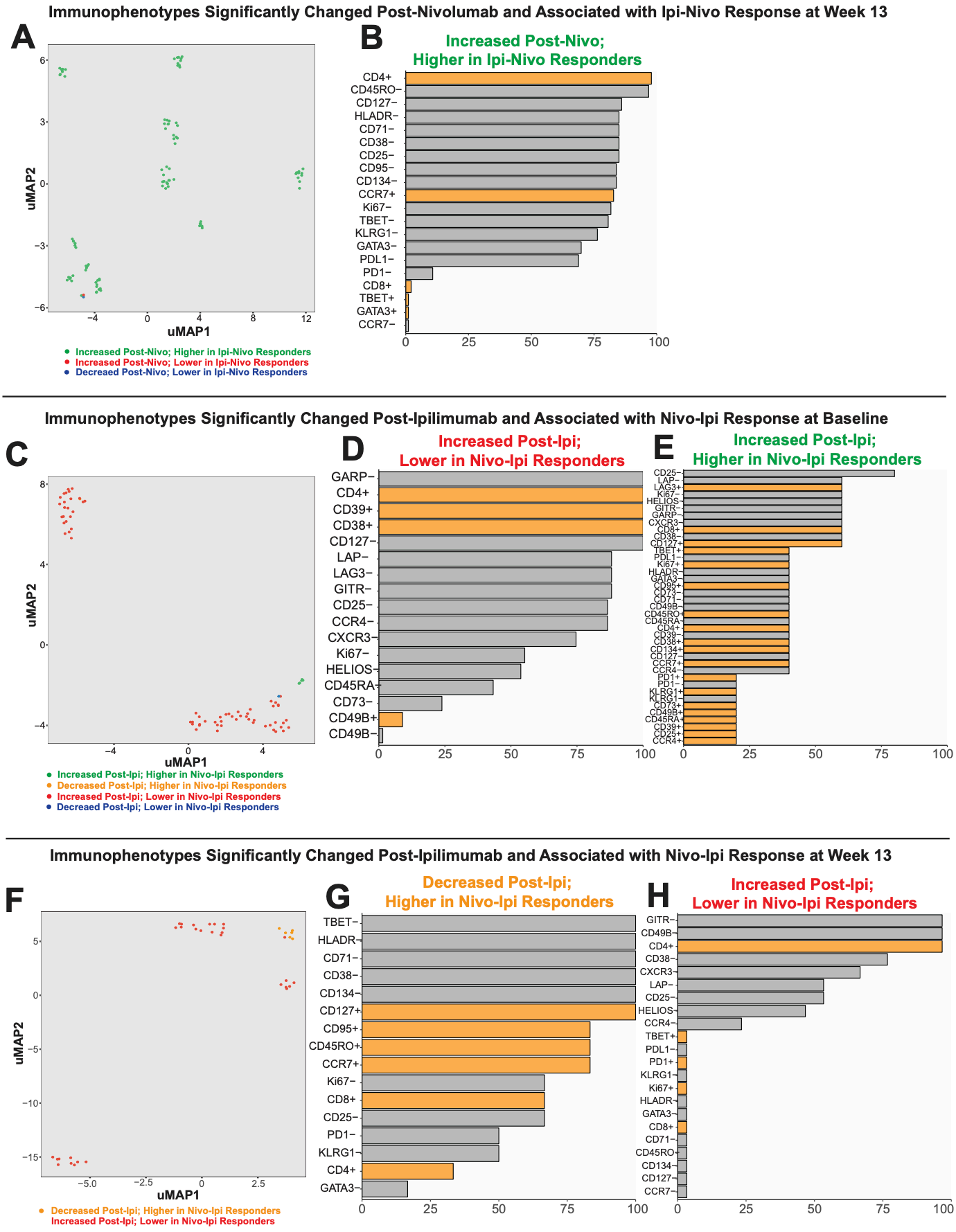

Supplemental Figure 8. Nivolumab or ipilimumab induced immunophenotypic changes overlapping with biomarkers of patient outcomes. (A) Immunophenotypes significantly changed post-nivolumab and associated with response/survival in ipilimumab>nivolumab treated patients at week 13 were reduced to a two-dimensional graph by UMAP by using frequency values for all patient samples as n-dimension variables. Clusters were determined by K-Means. Each dot represents an immunophenotype and is colored by directions of change after nivolumab and relative representation in ipilimumab>nivolumab responding patients. Immunophenotypes increasing post-nivolumab and higher in ipilimumab>nivolumab responding patients are shown in green. Immunophenotypes increasing post-nivolumab and lower in ipilimumab>nivolumab responding patients are shown in red. Immunophenotypes decreasing post-nivolumab and lower in ipilimumab>nivolumab responding patients are shown in green. **(B)** The frequency for all markers appearing in immunophenotypes increasing post-nivolumab and higher in ipilimumab>nivolumab responding patients are plotted. **(C)** Immunophenotypes significantly changed post-ipilimumab and associated with response/survival in nivolumab>ipilimumab treated patients at baseline are likewise plotted. **(D)** The frequency for all markers appearing in immunophenotypes increasing post-ipilimumab and lower in nivolumab>ipilimumab responding patients are plotted. **(E)** The frequency for all markers appearing in immunophenotypes increasing post-ipilimumab and higher in nivolumab>ipilimumab responding patients are plotted. **(F)** Immunophenotypes significantly changed post-ipilimumab and associated with response/survival in nivolumab>ipilimumab treated patients at week 13 are plotted as in A and C. **(G)** The frequency for all markers appearing in immunophenotypes decreased post-ipilimumab and higher in nivolumab>ipilimumab responding patients are plotted. **(H)** The frequency for all markers appearing in immunophenotypes increasing post-ipilimumab and lower in nivolumab>ipilimumab responding patients are plotted.

Supplemental Figure 9

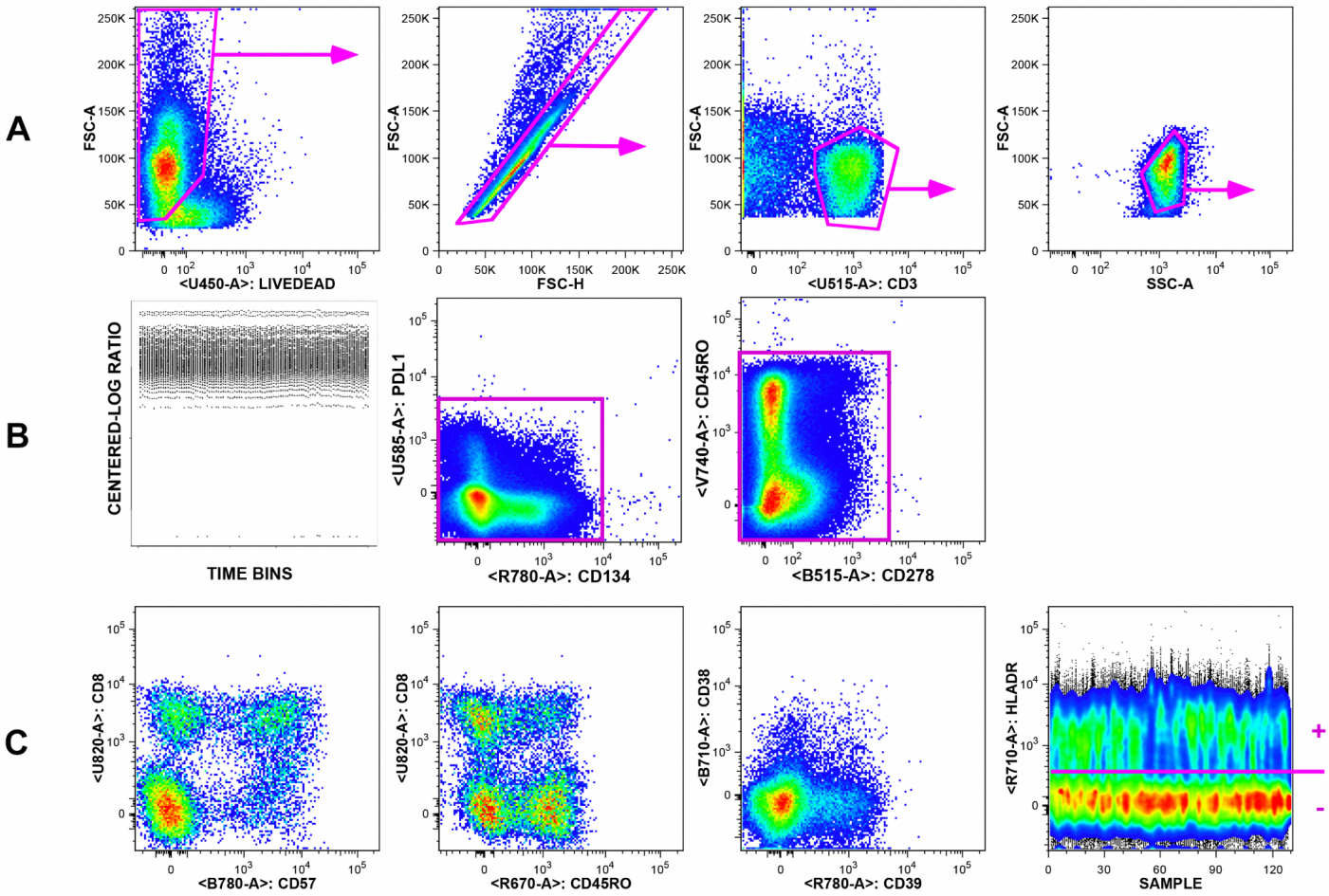

Supplemental Figure 9. Gating strategy and examples for high parameter flow cytometry panels. (A) Example of initial gating strategy for exclusion of dead cells using Live/Dead fixable dye, removal of doublets by examining forward scatter height (FSC-H) vs area (FSC-A), identification of CD3+ T-cells and lymphocytes (for those panels focused on these cells). **(B)** In the first panel, flowClean was used to examine each sample file for fluorescence anomalies associated with data acquisition on the high-throughput plate reader. No anomalies were detected. The second and third panels show examples of removal of fluorescence aggregates. **(C)** Staining patterns from representative samples were used to roughly identify a threshold gate that discriminates between cells expressing or lacking expression of a marker. These thresholds were confirmed by analyzing a concatenated file that included 10% of all events (randomly selected) from each sample. We included a parameter that discriminated each sample in the dataset, which is plotted on the x-axis of the final histogram in the figure. We examined each parameter on the y-axis, and placed the final threshold discriminating expression (+) and lack of expression (-) at a level appropriate for all samples in the dataset.

Supplemental Table.

Supplemental Table 1. Flow Cytometry Panels.

Directed Panel

Detector	Antibody	Fluorochrome	Clone	Vendor
B515	CD186	BB515	13B 1E5	BD Biosciences
B610	CD137	BB630	4B4-1	BD Biosciences
B670				
B710	CD244	CY55PERCP*	C1.7	BioLegend
B780	CD57	BB790	NK-1	BD Biosciences
G575	TIGIT	PE**	MBSA43	BD Biosciences
G610	CD272	CF594PE	J168-540	BD Biosciences
G670	CD127	CY5PE*	A019D5	BioLegend
G710				
G780	CD152	CY7PE**	L3D10	BioLegend
R670	CD45RO	APC*	UCHL1	BioLegend
R710	HLADR	R700APC	G46-6	BD Biosciences
R780	GITR	APCFIRE750*	108-17	BioLegend
U380	CCR7	BUV395	150503	BD Biosciences
U450	LD BLUE		N/A	Thermo
U515	CD3	BUV496	UCHT1	BD Biosciences
U585	CD25	BUV563	2A3	BD Biosciences
U670	CD366	BUV661	7D3	BD Biosciences
U740				
U820	CD8	BUV805	RPA-T8	BD Biosciences
V420	CD278	BV421	DX29	BD Biosciences
V475	CD95	BV480	DX2	BD Biosciences
V585				
V610	CD103	BV605	BER-ACT8	BD Biosciences
V670	CD183	BV650*	G025H7	BioLegend
V710	CD134	BV711	L106	BD Biosciences
V740	CD69	BV750	FN50	BD Biosciences
V780	CD4	BV786	EH12.2H7	BioLegend

T-cell Checkpoint Panel

Detector	Antibody	Fluorochrome	Clone	Vendor
B515	CD278 (ICOS)	BB515	DX29	BD Biosciences
B610	CD95	BB630	DX2	BD Biosciences
B670	KLRG1	BB660	MAFA	BD Biosciences
B710	CD127	BB700	HIL-7R-M21	BD Biosciences
B780	CCR7	BB790	3D12	BD Biosciences
G575	PD1	PE	MIH4	BD Biosciences
G610	KI67	CF594PE	B56	BD Biosciences
G670	HLADR	CY5PE	G46-6	BD Biosciences
G710				
G780	EOMES	CY7PE**	DAN11MAG	Thermo
R670	TBET	E660**	4b10	Thermo
R710	CD28	R700APC	CD28.2	BD Biosciences
R780	CD134	CY7APC	BerACT35	BD Biosciences
U380	CD137	BUV395	4B4-1	BD Biosciences
U450	LD BLUE		N/A	Thermo
U515				
U585	PDL1	BUV563	MIH1	BD Biosciences
U670	GATA3	BUV661	L50-823	BD Biosciences
U740	PD1	BUV737	MIH4	BD Biosciences
U820	CD71	BUV805	M-A712	BD Biosciences
V420	CD25	BV421	M-A251	BD Biosciences
V475	CD38	BV510*	HIT2	Biolegend
V585	CD3	BV570	UCHT1	BD Biosciences
V610	CD8	BV605*	RPA-T8	Biolegend
V670	CD4	SB645**	RPA-T4	Thermo
V710	FOXP3	BV711	259D/C7	BD Biosciences
V740	CD45RO	BV750	UCHL1	BD Biosciences
V780	CD19	BV786	HIB19	BD Biosciences
	CD14	BV786	M5E2	BD Biosciences
	CD56	BV786	B159	BD Biosciences

Checkpoint Ligand Panel

Detector	Antibody	Fluorochrome	Clone	Vendor
B515	CD206	BB515	19.2	BD Biosciences
B610				
B670				
B710	CD66B	CY55PERCP	G10F5	BD Biosciences
B780	CD4	BB790	RPA-T4	BD Biosciences
G575	GAL9	PE	9M1-3	BD Biosciences
G610	CD15	CF594PE	HI98	BD Biosciences
G670	HLA-DR	CY5PE	G46-6	BD Biosciences
G710				
G780	CD40	CY7PE	5C3	BD Biosciences
R670	CD163	AF647	GHI/61	BD Biosciences
R710	CD86	AF700	2331	BD Biosciences
R780	CD80	H7APC	L307.4	BD Biosciences
U380	PDL2	BUV395	MIH18	BD Biosciences
U450	LD BLUE		N/A	Thermo
U515	CD3	BUV496	UCHT1	BD Biosciences
U585	CD56	BUV563	NCAM16.2	BD Biosciences
U670	CD11C	BUV661	B-ly6	BD Biosciences
U740	CD19	BUV737	SJ25C1	BD Biosciences
U820	CD14	BUV805	M5E2	BD Biosciences
V420	OX40L	BV421	ik-1	BD Biosciences
V475	CD11B	eBio EF506	M1/70	Thermo
V585				
V610	41BBL	BV605 BD	C65-485	BD Biosciences
V670	CD33	BV650	WM53	BD Biosciences
V710	ICOSL	BV711	2D3/B7-H2	BD Biosciences
V740				
V780	PDL1	BV786	MIH1	BD Biosciences

Regulatory T-cell Panel

Detector	Antibody	Fluorochrome	Clone	Vendor
B515	CD25	FITC*	M-A251	Biolegend
B610				
B670	CD49B	BB660	12F1	BD Biosciences
B710	CD38	BB700	HIT2	BD Biosciences
B780	CD45RA	BB790	HI100	BD Biosciences
G575	CD194 (CCR4)	PE**	D8SEE	BD Biosciences
G610	KI67	CF594PE	B56	BD Biosciences
G670	LAG3	PE-CY5	T47-530	BD Biosciences
G710				
G780	CTLA4 (CD152)	CY7PE**	14D3	Thermo
R670	GARP	APC*	7B11	Biolegend
R710	CD8	R700APC	RPAT8	BD Biosciences
R780	CD39	CY7APC	TU66	BD Biosciences
U380	IDO	BUV395	V50-1886	BD Biosciences
U450	LD BLUE		N/A	Thermo
U515	HELIOS	BUV496	22F6	BD Biosciences
U585				
U670	CD3	BUV661	UCHT1	BD Biosciences
U740				
U820	CD73	BUV805	AD2	BD Biosciences
V420	FOXP3	BV421	259D/C7	BD Biosciences
V475	CXCR3	BV480	1C6/CXCR3	BD Biosciences
V585	LAP	BV570	TW4-2F8	BD Biosciences
V610	CD4	BV605	RPA-T4	BD Biosciences
V670	GITR	BV650	V27-580	BD Biosciences
V710				
V740				
V780	CD127	BV786	HIL-7R-M21	BD Biosciences